

Provided by the author(s) and University of Galway in accordance with publisher policies. Please cite the published version when available.

Title	A stainless steel multi-well plate (SS-MWP) for high-throughput Raman analysis of dilute solutions
Author(s)	Ryder, Alan G.; Li, Boyan; Ryan, Paul W.; Sirimuthu, Narayana M. S.
Publication Date	2010
Publication Information	Ryder, A.G., De Vincentis, J., Li, B., Ryan, P.W., Sirimuthu, N.M.S., Leister, K.J. (2010) 'A stainless steel multi-well plate (SS-MWP) for high-throughput Raman analysis of dilute solutions'. Journal Of Raman Spectroscopy, 41 (10):1266-1275.
Publisher	Wiley
Link to publisher's version	<a href="http://dx.doi.org/10.1002/jrs.2586">http://dx.doi.org/10.1002/jrs.2586</a>
Item record	<a href="http://hdl.handle.net/10379/2981">http://hdl.handle.net/10379/2981</a>
DOI	<a href="http://dx.doi.org/DOI 10.1002/jrs.2586">http://dx.doi.org/DOI 10.1002/jrs.2586</a>

Downloaded 2024-05-18T00:46:07Z

Some rights reserved. For more information, please see the item record link above.



# A STAINLESS STEEL MULTI-WELL PLATE (SS-MWP) FOR HIGH THROUGHPUT RAMAN ANALYSIS OF DILUTE SOLUTIONS.

Alan G. Ryder,<sup>1,2\*</sup> John de Vincentis,<sup>3</sup> Boyan Li,<sup>1,2</sup> Paul W. Ryan,<sup>1,2</sup> Narayana M. S. Sirimuthu,<sup>1,2</sup> and Kirk J. Leister.<sup>3</sup>

<sup>1</sup> Nanoscale Biophotonics Laboratory, School of Chemistry, National University of Ireland, Galway, Galway, Ireland.

<sup>2</sup> Centre for Bioanalytical Sciences, School of Chemistry, National University of Ireland, Galway, Galway, Ireland.

<sup>3</sup> Bristol-Myers Squibb, Process Analytical Sciences, Syracuse, New York, USA.

\* To whom all correspondence should be addressed.

**Tel:** +353 91 49 2943 **Fax:** +353 91 49 4596 **Email:** alan.ryder@nuigalway.ie (A.G.R)

**Published Citation:** A Stainless Steel Multi-Well Plate (SS-MWP) for High Throughput Raman Analysis of Dilute Solutions. A.G. Ryder, J. De Vincentis, B. Li, P.W. Ryan, N.M.S. Sirimuthu, and K.J. Leister. *Journal of Raman Spectroscopy*, 41(10), 1266-1275, (2010).

**DOI:** <http://dx.doi.org/10.1002/jrs.2586>

**Note:** This is the final accepted version that includes all proofing corrections. The final definitive version of the manuscript is available on the Macromolecules website.

## Abstract:

The use of Raman spectroscopy for the qualitative and quantitative analysis of dilute aqueous solutions is of interest to the biopharmaceutical manufacturing sector. However, the inherent weakness of the Raman effect, coupled with spectral variability due to spurious signals from sample holders can produce significant problems for chemometric based high throughput assays. Therefore, there is a need for a multi-well sample holder that ensures robust and repeatable measurements in particular from dilute aqueous solutions such as cell culture media. Here we demonstrate the efficacy of a novel, electropolished, stainless steel multi-well plate (SS-MWP) sample holder with 96 wells for dilute aqueous solution analysis. A comprehensive study of spectroscopic behaviour was carried out and comparisons made with multi-well plates fabricated from polystyrene, polypropylene, and aluminium. A key factor in the validation studies is the use of intrinsically weak Raman scattering systems e.g. water and dilute glucose solutions. The data collected show that the SS-MWP are much superior in terms of robustness, resistance to chemical attack, and measurement reproducibility and as such are the ideal sample holders for Raman analysis of dilute solutions.

**Keywords:** Raman spectroscopy, sample holder, similarity analysis, aqueous solution, high throughput.

## 1. Introduction

Raman spectroscopy is a versatile technique for the analysis of solid and liquid materials: because of the high information content in the spectra and the non-contact, non-destructive measurement methodology.<sup>1-6</sup> The minimal sample preparation required also makes this technique suitable for high-throughput analysis. Furthermore, the detail in Raman spectra provides information on the molecular properties and composition of the sample which can be used for identification and quality control purposes.<sup>7, 8</sup> When combined with chemometric data analysis, Raman spectroscopy also enables accurate quantitative assessment of the chemical composition of complex mixtures. The continual development of instrumentation and chemometric tools, has advanced the analysis of increasingly complex samples in many different application areas.<sup>1, 2, 9</sup>

One of the key challenges for Raman spectroscopy as an analytical tool is in the analysis of dilute aqueous solutions, such as the complex cell culture media used in biopharmaceutical manufacturing processes. These samples typically contain dozens of analytes, all of which are present in low concentrations, with typical dissolved solids concentration of 1-2% (by weight) or less. At these low concentrations, the water signal is very significant and the analyte bands in the Raman spectra are usually very weak. Thus, if one wishes to implement Raman based methods, one has to pay particular attention to the quality of the spectral data that are collected. The most common sample holders utilised for high throughput sampling (HTS) are the ubiquitous, low cost, polystyrene, and polypropylene multi-well plates.<sup>10</sup> However, two factors which contribute to signal variability (and thus efficacy of chemometric based analyses) are the focal volume sampled, and the relative intensities of the holder material versus the analyte. For HTS, one typically does not use confocal optics and therefore the focal volumes tend to be relatively large, and thus the Raman spectrum will be generated from a significant sample volume. If the focal volume overlaps the bottom of the sample well, then some of the signal will originate from the material used to fabricate the sample holder. Now the second factor becomes an issue, because, for example with polymeric based holders, the more crystalline and denser the polymer, the stronger the Raman signal in comparison to the weak signal from the aqueous sample. A similar problem is also encountered with the use of glass or quartz substrates, and so one has to consider the use of metallic sample holders which will not contribute to the Raman signal. Other considerations with regard to sample holder design include resistance to chemical attack and thermal transfer. Polymer based holders are obviously unsuited to organic solvents, while glass or quartz can yield background signal contamination. Metal samples holders, such aluminium crucibles or multi-well plates can be corroded by highly acidic samples, such as some supplements used for cell culture media formulation.

Here we describe an ideal solution, an electropolished, stainless steel 96 multi-well plate (SS-MWP) which is particularly suitable for HTS measurement of dilute solutions. A comprehensive spectroscopic study in terms of background effect, sample volume effect, response linearity and well-to-well variability was undertaken by using water and glucose solutions. The performance of the SS-MWP was compared with that from aluminium, polystyrene, and polypropylene 96 multi-well plates. Spectral performance was assessed using a variety of chemometric methods including similarity analysis,<sup>11-13</sup> multivariate analysis of variance (MANOVA)<sup>14, 15</sup> and partial least-squares (PLS) regression.<sup>16, 17</sup> The data show clearly that these stainless steel sample holders are the ideal solution for the HTS Raman of dilute aqueous solutions.

## **2. Materials and Methods**

### *2.1 Materials*

The stainless steel and aluminium plates were manufactured by Akreturn Manufacturing Inc (<http://www.akreturn.com/>) using conventional methods and the SS-MWP was fabricated from 316 stainless steel and then electropolished to provide a mirror finish and good protection against chemical attack. The aluminium 96 multi-well plate was fabricated from 6061 aluminium and hard anodized. In both cases, the wells were 6.2 mm in diameter with a depth of 8.0 mm, giving a well capacity of ~230  $\mu\text{L}$ . Figure 1 shows photographs and an engineering drawing of the multi-well plates showing the curved well bottom. The polypropylene 96 deep well plates (SMI-LabHut Ltd, UK) had wells of 7.0 mm in diameter, which were flat bottomed, and had a depth of 11.0 mm, giving a well capacity of ~392  $\mu\text{L}$ . The polystyrene microtitre 96 deep well plates were obtained from Corning, Inc., US and the wells were round bottomed, 7.0 mm in diameter with a depth of 11.0 mm, giving a well capacity of ~390  $\mu\text{L}$ .

ACS reagent grade D-glucose was purchased from Sigma-Aldrich, Inc., and a 40.0 g/L solution was prepared by dissolving 2.0 g of solid glucose in 50 mL Millipore water.

## 2.2 Instrumentation and data collection

Raman measurements were recorded at room temperature using a Raman spectrometer (AVALON Instruments Ltd, UK) equipped with a 785 nm laser diode excitation and a TE cooled (-90 °C) back thinned CCD detector. The system is fitted with a motorised XYZ sample stage which accepts standard sized multi-well plates. A laser power of ~70 mW (at the sample) with an exposure time of  $2 \times 10$  seconds was generally used and spectra were collected from 250 to 3311  $\text{cm}^{-1}$  (at a resolution of 8  $\text{cm}^{-1}$ ). In the context of dilute sample analysis, the laser focus position is critical so as to minimise background effects and in this study, the integral autofocus mode was used for all measurements.

A background was taken at start of each collection and a deionised water spectrum was also measured at the beginning and end of each sequence of data collection. For each sample, the requisite volume was pipetted into a well and multiple Raman spectra collected using a  $3 \times 3$  grid (0.5 mm point spacing). An average spectrum was then generated from the nine individual grid spectra and used for all chemometric analyses.

## 2.3 Data analysis

The PerkinElmer Spectrum software version 6.3.1 was employed for data acquisition and initial evaluation of spectral properties and signal quality. All calculations were performed using the MATLAB platform version 7.4 (The MathWorks, Inc., US) on a standard PC (2.8 GHz Pentium D, Dell Optiplex PC, 1.0 GB RAM, Microsoft Windows XP OS). For the majority of the chemometric analyses undertaken, PLS\_Toolbox 4.0 (Eigenvector Research, Inc., US) and an in-house-written set of codes entitled "*Raman\_Toolbox*" were used. The *Raman\_Toolbox* (Nanoscale Biophotonics Laboratory, NUIG, Ireland) is a package of advanced functions that operate within the MATLAB computational environment and is used to speed up and simplify the data analysis workflow for large spectral datasets. It contains tools to load SP-, SPC-, or ASCII-format spectra and facilitates the construction of database as well as aiding data pre- and post-processing and the building of predictive models.

## 2.4 Similarity analysis

One of the key criteria used to judge the efficacy of the sample holders is to determine if spectra of a sample analyte, taken at different times and locations are identical, and this can be best achieved using chemometric methods. Here we used the Pearson product-moment correlation coefficient ( $Sr$ )<sup>11, 12</sup>, to calculate the similarity between two spectral observations  $\mathbf{x}_1$  and  $\mathbf{x}_2$  at  $m$  different Raman wavenumbers:

$$Sr(\mathbf{x}_1, \mathbf{x}_2) = \frac{(\mathbf{x}_1 - \bar{\mathbf{x}}_1)(\mathbf{x}_2 - \bar{\mathbf{x}}_2)^T}{\|\mathbf{x}_1 - \bar{\mathbf{x}}_1\|_p \|\mathbf{x}_2 - \bar{\mathbf{x}}_2\|_p} \quad (1)$$

The subscript  $p$  indicates the Entry wise  $p$ -norm. In this study it represents the 2-norm/Frobenius norm, i.e.,  $p=2$ . The superscript  $T$  denotes the transpose of the vector.  $\bar{\mathbf{x}}_1$  and  $\bar{\mathbf{x}}_2$  are mean vectors of  $\mathbf{x}_1$  and  $\mathbf{x}_2$ , respectively.

Another popular method used for similarity analysis is vector similarity  $Sv$ ,<sup>13</sup>

$$Sv(\mathbf{x}_1, \mathbf{x}_2) = 1 - \frac{\sum \|\mathbf{x}_1 - \mathbf{x}_2\|_p}{\sum \|\mathbf{x}_1 + \mathbf{x}_2\|_p} \quad (2)$$

where  $(\mathbf{x}_1 - \mathbf{x}_2)$  and  $(\mathbf{x}_1 + \mathbf{x}_2)$  respectively denote the difference and sum vectors between the two observations  $\mathbf{x}_1$  and  $\mathbf{x}_2$ . Note that in this case  $p=1$ , which means that the absolute modulus is executed on the individual elements of  $(\mathbf{x}_1 - \mathbf{x}_2)$  and  $(\mathbf{x}_1 + \mathbf{x}_2)$  prior to summation.

These similarity values reveal the extent to which two objects  $\mathbf{x}_1$  and  $\mathbf{x}_2$  correlate and the closer the similarity coefficient is to 1 (for  $Sr$  and  $Sv$ ), the more similar  $\mathbf{x}_1$  and  $\mathbf{x}_2$  are with respect to their spectral profiles. The correlation coefficient measures the linear correlation degree of  $\mathbf{x}_1$  and  $\mathbf{x}_2$ , whereas the vector similarity measures the percent of the common parts of two objects  $\mathbf{x}_1$  and  $\mathbf{x}_2$ , be they linearly or non-linearly correlated. The main outcome of this difference is that the vector similarity  $Sv$  is less influenced by baseline effects and is therefore more applicable to spectra with large baseline fluctuations.

## 2.5 Variance analysis

In terms of the present study, detailed variance analysis methods are used to quantify the variance due to different sample holders. The within-class variance is used to test well-to-well variability from repeated measurements on the same sample holder and the relative within-class variance is also used to test the reproducibility of repeated measurements, while the between-class variance is used to test for differences between different holders. These within-class variance and between-class variance are standard multivariate analysis of variance (MANOVA) methods that are used to describe the degree of relationship between a set of spectra (variables).<sup>14, 15</sup> The within-class variance ( $MS_w$ ) and between-class variance ( $MS_b$ ) are defined as follows:

$$MS_w = \frac{\sum diag((\mathbf{X} - \bar{\mathbf{X}})^T (\mathbf{X} - \bar{\mathbf{X}}))}{N-1} \quad (3)$$

$$MS_b = \frac{\sum diag((\bar{\mathbf{X}}_1 - \bar{\mathbf{X}}_{12})^T (\bar{\mathbf{X}}_1 - \bar{\mathbf{X}}_{12})) + \sum diag((\bar{\mathbf{X}}_2 - \bar{\mathbf{X}}_{12})^T (\bar{\mathbf{X}}_2 - \bar{\mathbf{X}}_{12}))}{N_1 + N_2 - 2} \quad (4)$$

where  $\mathbf{X}$  signifies a  $N \times m$  spectral response matrix of one class whose  $n^{\text{th}}$  row  $\mathbf{x}_n$  is the spectrum of the  $n^{\text{th}}$  observation.  $\bar{\mathbf{X}}$  is the mean matrix of  $\mathbf{X}$  which is of same size.  $(\mathbf{X} - \bar{\mathbf{X}})^T (\mathbf{X} - \bar{\mathbf{X}})$  is the cross-product matrix of the difference matrix  $(\mathbf{X} - \bar{\mathbf{X}})$ .  $diag((\mathbf{X} - \bar{\mathbf{X}})^T (\mathbf{X} - \bar{\mathbf{X}}))$  is a vector of

variances for each variable of  $\mathbf{X}$ . The superscript T denotes the matrix transpose.  $\mathbf{X}_1$  and  $\mathbf{X}_2$  are the spectral response matrices of two different classes, whose sizes are  $N_1 \times m$  and  $N_2 \times m$  respectively, and  $\bar{\mathbf{X}}_1$  and  $\bar{\mathbf{X}}_2$  are the respective mean matrices.  $\bar{\mathbf{X}}_{12}$  specifies a common mean matrix of both  $\mathbf{X}_1$  and  $\mathbf{X}_2$ , whose size can be  $N_1 \times m$  or  $N_2 \times m$  depending on the size of the  $\bar{\mathbf{X}}_1$  or  $\bar{\mathbf{X}}_2$  matrices already in use. A relative within-class variance ( $RMS_w$ ) can then be calculated as follows,

$$RMS_w = \frac{\sum \text{diag}((\mathbf{X} - \bar{\mathbf{X}})^T (\mathbf{X} - \bar{\mathbf{X}}))}{\sum \text{diag}(\mathbf{X}^T \mathbf{X})} \times 100\% \quad (5)$$

## 2.6 Partial least squares regression (PLS)

The final chemometric characterisation, involves determining the efficacy of the sample holders for quantitative measurements using PLS. PLS regression is well known and is most commonly used to formulate linear relationships between the spectral data and analyte concentrations.<sup>16, 17</sup> In assessing the quality of PLS calibration models, the root mean square error of calibration (RMSEC), equation 6, is a frequently used measure of the average difference between the predicted and measured response values at the calibration stage once the appropriate underlying components or latent variables (LVs) are determined, whilst the root mean square error of validation (RMSEV) is commonly employed at the validation stage.

$$\text{RMSEC} = \sqrt{\frac{(\hat{\mathbf{c}}_{\text{cal}} - \mathbf{c}_{\text{cal}})^T (\hat{\mathbf{c}}_{\text{cal}} - \mathbf{c}_{\text{cal}})}{N_{\text{cal}}}} \quad (6)$$

where the subscript 'cal' refers to the calibration set and the '^' indicates the concentration estimate.  $N_{\text{cal}}$  is the number of samples in the calibration set.

## 3. Results and Discussion

As part of an extended analytical chemistry research programme involving the development of novel analytical techniques for the biopharmaceutical manufacturing industry (specifically the manufacture of a recombinant protein using mammalian cell culture), we have had to analyse many thousands of dilute aqueous mixtures using Raman spectroscopy. The seemingly trivial problem of how to actually present large numbers of samples comprising of dilute, aqueous solutions in small volumes to the Raman spectrometer in such a way as to ensure highly reproducible measurements suitable for robust chemometric analysis had to be addressed. Initially, we used single-use, aluminium micro crucibles that were originally designed for Thermogravimetric Analysis (2 mm depth, ~50  $\mu\text{L}$  capacity, Thorn Scientific Services Ltd, UK). However, in some cases these were corroded by acidic samples, yielding anomalous Raman spectra. Platinum crucibles (4 mm depth, 80  $\mu\text{L}$  capacity, also from Thorn Scientific Services Ltd, UK) were tried, and while they produced good spectra, they were very expensive and impractical for high throughput sampling (HTS). This then led to the design and manufacture of stainless steel and aluminium multi-well plates (MWP), suitable for HTS.

### 3.1 Background & noise effects

To demonstrate the effect of Raman signal contamination from the MWP sample holders, Raman spectra of small volumes (100  $\mu$ L) of both water and glucose solution (40.0 g/L) were collected from the stainless steel, aluminium, polystyrene, and polypropylene multi-well plates. For each 100  $\mu$ L sample of water or glucose solution, nine Raman spectra were collected (Figure 2).

From Figure 2 it is clear, first of all, that for dilute aqueous solutions there are considerable baseline effects and variance in the O-H stretch band (strong band above  $\sim 3000$   $\text{cm}^{-1}$ ). This later variation arises from a combination of three main factors, the strong O-H stretch vibration, lower detector sensitivity above 1000 nm, and higher detector noise. However, for most analyses we have been developing, this spectral region can be safely discarded. The second important point is the presence of spurious bands in the spectra measured from samples held in polymer based multi-well plates. This is particularly evident for the polystyrene plates (Figure 2c) with relatively strong polystyrene peaks at 1003  $\text{cm}^{-1}$ , 1195  $\text{cm}^{-1}$ , 1604  $\text{cm}^{-1}$  and 2910  $\text{cm}^{-1}$ . The polypropylene plates (Figure 2d) also generate strong, substrate peaks at 812  $\text{cm}^{-1}$ , 1460  $\text{cm}^{-1}$ , and 2886  $\text{cm}^{-1}$ . Conversely, the stainless steel and aluminium MWP sample holders show no spurious peaks in the spectra of either the water or glucose solution. The magnitude of these substrate bands in relation to the water and glucose bands is also a potential more significant problem when one considers the manner in which Raman autofocus algorithms are implemented. If an autofocus algorithm operates on the integrated full Raman spectrum, then it is possible (and we have observed this) that the instrument will interpret the substrate signal as analyte signal thus causing a greater overlap of the focal into the sample holder substrate material. In automated HTS applications this is obviously a serious problem, but which is negated by the use of the metal holders.

A third important facet about the analysis of dilute solutions is the large contribution from the water solvent. The O-H stretch region shows the largest variation and noise, but it can usually be disregarded in chemometric modelling as the 2500–4000  $\text{cm}^{-1}$  region does not contribute significantly to information content. However, in the fingerprint region, the two broad bands at  $\sim 1364$   $\text{cm}^{-1}$  and  $\sim 1636$   $\text{cm}^{-1}$  will always make a significant contribution to the Raman spectra of dilute aqueous solution samples. Variances in these bands due to sample holder effects will cause significant errors in chemometric modelling, particularly where they overlap with analyte bands.

To clarify the root causes of sample spectral variance, it is therefore necessary to remove both the baseline effects and the water signal. Therefore, for each sample, the nine individual spectra with treated with a multiplicative scatter correction (MSC), then averaged to produce a single spectrum. However, the MSC method does not remove the sloping background so we then implemented an asymmetric weighted least squares algorithm<sup>18</sup> to remove the remaining baseline effects. Finally an orthogonal projection method<sup>19</sup> was used to subtract the water signal from the spectra prior to chemometric analysis.

Figure 3 shows the background-subtracted Raman spectra for the glucose solutions (40 g/L) measured in the different sample holders. This data transformation reduces the spectral variance due to the water and makes the analyte bands much clearer, particularly in the fingerprint region (274–1604  $\text{cm}^{-1}$ ).

To quantify the degree of difference in the Raman spectra collected from the four different MWP sample holders, the nine Raman spectra collected for each glucose solution, shown in Figures 2 (before background subtraction) and 3 (after background subtraction), were first averaged to generate a single spectrum. Then, using equations (1) and (2) the similarity coefficients  $S_r$  and  $S_v$  were calculated for the resulting spectra (274–1604  $\text{cm}^{-1}$  region). The 96 well SS-MWP was used as the reference for these calculations (Table 1).

The similarity coefficients calculated using the raw data show clearly that the spurious peaks originating from the PS-MWP have a significant, quantifiable, negative effect. The low values obtained for the Al-MWP are a bit surprising, but can however be explained by the presence of larger background/baseline fluctuations in spectra collected from the Al-MWP which has a matt finish. Therefore the Al-MWP spectra before background subtraction are significantly different to those collected from the SS-MWP. As mentioned earlier,  $S_v$  is less susceptible to the influence of background which accounts for its higher value in this instance. Upon removal of the background the Al-MWP spectra provide more acceptable similarity values which represent differences due to the Raman signals rather than background/baseline effects. The PP-MWP performs quite well because the polypropylene substrate is less crystalline compared to polystyrene, and as a consequence the Raman scattering is considerably weaker. The background subtraction improves the coefficient values significantly, but it is still very obvious that the PS-MWP, is worse because of the contaminant bands from the polystyrene substrate. Figure 3e shows the background-subtracted Raman fingerprint region spectra for the SS-MWP, Al-MWP, and PP-MWP sample holders while Figure 3f shows a comparison of the PS-MWP and SS-MWP sample holders. Particular attention should be paid to a prominent contaminant band appearing around  $1003\text{ cm}^{-1}$  in the PS-MWP spectral profile. The results presented in table 1 show that the correlation coefficient ( $S_r$ ) tends to give higher values than the vector similarity ( $S_v$ ) once the background is removed from the spectral data. Therefore,  $S_v$  is preferred for a more reliable determination of how similar or correlated two measurements may be as it provides more sensitive assessments and is more resistant to the influence of background/baseline effects.

### 3.2 Performance analysis of SS-MWP

The overall performance of the stainless steel 96 deep well plate can be assessed under a number of criteria: signal intensity, sample volumes, well to well variability, and linearity of response with respect to concentration in a dilute solution.

#### 3.2.1 Signal intensity

A second significant advantage of the SS-MWP is that the intensity of the Raman spectra is at least twice that collected from the standard polymer multi-well plates (Figure 2). This is due to the high surface reflectivity of the electropolished SS-MWP which reflects the excitation light back through the sample and also concentrates and reflects back a larger proportion of the Raman signal. This is a significant advantage when dealing with weakly scattering samples. The aluminium plates which are of a matt finish do not perform as well as the stainless steel, with signal intensities being significantly lower.

#### 3.2.2 Volume effects

One of the potential problems faced in biopharmaceutical analysis is the fact that samples may only be available in small quantities and/or volumes. Thus it was important to determine the optimal sample volumes for use with the SS-MWP that yield reproducible data. In the first test, the Raman spectra of different volumes (40  $\mu\text{L}$ , 80  $\mu\text{L}$ , 100  $\mu\text{L}$ , 150  $\mu\text{L}$  and 200  $\mu\text{L}$ ) of water (Figure 4) and 40 g/L glucose solution (Figure 5) were each measured three times from different wells.

Similarity coefficients were also calculated from the volume measurements described above and the 100  $\mu\text{L}$  water measurement was used as the reference spectrum. After averaging the nine traces from each water measurement, baseline correction was applied and the resulting Raman spectra in the  $250\sim 2525\text{ cm}^{-1}$  region were utilised for the similarity calculations (Table 2). All of the calculated similarity values approach unity indicating that the five measurements are nearly



identical, and so the volume effect is negligible on the baseline corrected Raman spectra collected from the SS-MWP.

Figures 4 and 5 show high variability above  $\sim 2700\text{ cm}^{-1}$  and strong water band contributions, which as previously noted necessitates removal of the water background. The first point of note is that the high wavenumber range always shows a large variation, and is thus a spectral area that should not be used for quantitative measurement. The second notable point is that there is always some degree of baseline fluctuation between wells, irrespective of the sample solution volume. This necessitates the implementation of baseline correction prior to any chemometric data analysis. Once baseline corrected, the spectra collected from different volumes show improved overlap as is evident from Figure 4b and Figure 5e. Figure 5f shows such background subtracted spectra in the fingerprint region.

For the glucose solution measurements, a similarity analysis was applied to the background subtracted Raman spectra. Figure 6 provides an overview of the resulting similarity values and reveals that there is a good consistency of performance amongst the different stainless steel plate wells with regard to Raman measurement of the different volumes of glucose solution. As previously discussed, the  $S_r$  values show less variation while the  $S_v$  value shows a greater distribution. For these types of measurement where the analyte signals are very weak, the use of the  $S_v$  value is preferred as it can highlight the subtle differences in the spectra, which can adversely affect the performance of chemometric models.

### 3.2.3 Well-to-well variability

In order to robustly evaluate the well-to-well variability of the SS-MWP, 100  $\mu\text{L}$  of 40.0 g/L glucose solution was pipetted into 40 random wells in each of three individual plates (120 total). Raman measurements were then taken from all 120 wells (Figure 7) and it is clear that baseline drift and spectral fluctuations are significant issues. The spectra were then baseline corrected, water signal removed, first order derivatised and infinity normalised before undertaking a variance analysis in terms of the within-class, relative within-class and between-class variances using equations (3), (4) and (5). Table 3 shows the results of these variance analyses. The relative within-class variances ( $RMS_w$ ) obtained from the different wells on same plate are all very low, i.e., 0.134% for the SS-MWP1, 0.402% for the SS-MWP2, and 0.353% for the SS-MWP3, and thus ensures reproducible measurements irrespective of the particular well or plate chosen. The within-class variances can be seen from Table 3 to be much larger than the between-class variances. For instance, the within-class variance ( $MS_w$ ) of the SS-MWP2 is 0.0527, 44 times the between-class variance ( $MS_b=0.0012$ ) of the SS-MWP2 and SS-MWP3. This is a result of the inherent sensitivity of the within-class variance algorithm rather than any sample holder discrepancy. The within-class variance algorithm assumes a normal random distribution of measurement residuals and provides a quantitative measurement of this total variance. On the other hand the between class variance algorithm essentially correlates the variance distribution patterns of two different classes and describe the degree of relationship between them. Therefore, it is not surprising that the between class variance values presented in Table 3 are lower than the within class variances since the variance distributions for each of the SS-MWPs, if normal and random, are likely to be of similar magnitude, i.e. the fact that the between-class variance obtained from two SS-MWPs is significantly smaller than the within-class variances indicates that there is no significant difference between them with regard to well-to-well variability.

### 3.2.4 Linearity test

To further demonstrate efficacy of the SS-MWPs, the linearity response was measured by PLS modelling using eleven glucose solutions at various concentrations. The dilute solutions had concentrations between 0 and 40 g/L varying in 4 g/L increments, and the Raman data were collected from 200  $\mu$ L aliquots. A Raman spectrum of water was used as a blank background. Prior to PLS modelling, the Raman data were pre-processed by first averaging the nine spectra collected for each sample, baseline correction, background subtraction of the water spectrum, and finally first order, Savitzky-Golay derivative (Figure 8a).<sup>20</sup> A PLS model was built using the eleven measurements over the 274~1604  $\text{cm}^{-1}$  spectral range after the mean-centering was conducted on both the spectral responses and concentrations. Leave-one-out cross validation<sup>21, 22</sup> was utilised to select one underlying component with which the calibration model gives the minimum errors of RMSEV = 0.81 g/L and RMSEC = 0.70 g/L (Figure 8b). The single underlying component is quite interpretable, and it accurately represents the concentration of glucose in solution. The PLS model clearly shows that using the SS-MWPs, good quantitative correlations for dilute solutions of weak Raman scatterers can be obtained.

#### 4. Conclusions

Recent advances in Raman spectroscopic methods have made it an extremely attractive and viable option for the routine analysis of a wide range of low concentration analytes such as those prevalent in the biopharmaceutical industry due to its ability to analyse aqueous samples readily and extract useful quantitative information from the spectra. There is therefore a need for high throughput, robust, and reproducible methods for low concentration analytes, and thus one requires multi-well sample holders. The quantitative and qualitative analysis of dilute aqueous solutions by Raman spectroscopy is however, often a challenging proposition, and care must be taken to eliminate potential sources of error such as background signal originating from the materials from sample holders which can adversely affect performance.

In comparison to common polymer based multi-well sample holders, these new electropolished SS-MWPs show significant advantages, with higher spectral purity, more intense spectra, and better reproducibility for dilute aqueous solutions. These benefits arise from a combination of purely physical effects such as the metallic nature of the holder (no Raman bands), and from increased back reflection due to the highly polished well surfaces. The benefits of this SS-MWP for high throughput Raman analysis of low concentration analytes are undeniable and we have implemented their use for the analysis of a wide range of materials used for commercial cell culture media manufacturing.

#### 5. Acknowledgements

This work was funded by Bristol-Myers Squibb and the Irish Industrial Development Authority (IDA) under the Centre for Bioanalytical Sciences (CBAS) programme which is a joint, collaborative research programme involving the National University of Ireland, Galway, Bristol-Myers Squibb, and Dublin City University.

#### 6. References

- [1] E. Smith, G. Dent, *Modern Raman Spectroscopy – A Practical Approach*, John Wiley & Sons, Chichester, **2005**.
- [2] S. P. Mulvaney, C. D. Keating, *Anal. Chem.*, **2000**, 72, 145R.
- [3] Z. Movasaghi, S. Rehman, I. U. Rehman, *Appl. Spectrosc. Rev.*, **2007**, 42, 493.

- [4] T. R. M. De Beer, M. Allesø, F. Goethals, A. Coppens, Y. V. Heyden, H. L. De Diego, J. Rantanen, F. Verpoort, C. Vervaet, J. P. Remon, W. R. G Baeyens, *Anal. Chem.*, **2007**, 79, 7992.
- [5] Z. Chen, G. Fevotte, A. Caillet, D. Littlejohn, J. Morris, *Anal. Chem.*, **2008**, 80, 6658.
- [6] S. Folestad, J. Johansson, *Am. Pharm. Rev.*, **2004**, 7, 82.
- [7] W. Kiefer, *J. Raman Spectrosc.*, **2007**, 38, 1538.
- [8] W. Kiefer, *J. Raman Spectrosc.*, **2007**, 39, 1710.
- [9] C. M. Harris, *Anal. Chem.*, **2003**, 75, 75A.
- [10] C. J. S. Pommier, V. Rosso, *Am. Pharm. Rev.*, **2005**, 8, 19.
- [11] J. L. Rodgers, W. A. Nicewander, *The American Statistician*, **1988**, 42, 59.
- [12] J. Cohen, P. Cohen, S. G. West, L. S. Aiken, *Applied Multiple Regression/Correlation Analysis for the Behavioral Sciences*, 3<sup>rd</sup> edn, Lawrence Erlbaum Associates, New Jersey, 2003.
- [13] P. Tan, M. Steinbach, V. Kumar, *Introduction to Data Mining*, Pearson Higher Education, Addison-Wesley, New Jersey, **2005**.
- [14] H. R. Barker, B. M. Barker, *Multivariate Analysis of Variance (MANOVA): A Practical Guide to Its Use in Scientific Decision-Making*, University of Alabama Press, Birmingham, **1984**.
- [15] C. J. Huberty, S. Olejnik, *Applied MANOVA and Discriminant Analysis*, 2<sup>nd</sup> edn., John Wiley & Sons, New Jersey, **2006**.
- [16] H. Martens, T. Naes *Multivariate Calibration*, 2<sup>nd</sup> edn., Wiley, New York, **1991**.
- [17] T. Naes, T. Isaksson, T. Fearn, T. Davies, *A User-Friendly Guide to Multivariate Calibration and Classification*, NIR Publications, Chichester, **2002**.
- [18] D. M. Haaland, R. G. Easterling, *Appl. Spectrosc.*, **1982**, 36, 665.
- [19] A. Lorber *Anal. Chem.*, **1986**, 58, 1167.
- [20] A. Savitzky, M.J.E. Golay, *Anal. Chem.*, **1964**, 36, 1627.
- [21] D. M. Allen, *Technometrics*, **1974**, 16, 125.
- [22] H A. Martens, P. Dardenne, *Chemom. Intell. Lab. Syst.* **1998**, 44, 99.

**Table 1:** Similarity coefficients calculated from Raman measurements of a 40 g/L glucose solution using the four MWP sample holders. Values were calculated relative to the spectra collected from the SS-MWP over the 274~1604  $\text{cm}^{-1}$  spectral region.

Sample holder	Before background subtraction		After background subtraction	
	$S_r$	$S_v$	$S_r$	$S_v$
Stainless steel MWP (SS-MWP)	1	1	1	1
Polypropylene MWP (PP-MWP)	0.956	0.962	0.986	0.936
Aluminium MWP (Al-MWP)	0.773	0.891	0.986	0.931
Polystyrene MWP (PS-MWP)	0.619	0.918	0.944	0.899

**Table 2:** Similarity coefficients for water measurements taken from different wells of SS-MWP. Baseline corrected Raman spectra over the 250~2525  $\text{cm}^{-1}$  region were used for calculation against the reference measurement (100  $\mu\text{L}$  water sample).

Water volume	$S_r$	$S_v$
40 $\mu\text{L}$	0.999	0.981
80 $\mu\text{L}$	1	0.989
100 $\mu\text{L}$	1	1
150 $\mu\text{L}$	1	0.992
200 $\mu\text{L}$	1	0.991

**Table 3:** Within and between-class variances obtained from Raman measurements of glucose solution from three different SS-MWPs.

Variance	SS-MWP1	SS-MWP2	SS-MWP3
$RMS_w$	0.134%	0.402%	0.353%
SS-MWP1	<b>0.0178*</b>	0.0078	0.0058
SS-MWP2	0.0078	<b>0.0527*</b>	0.0012
SS-MWP3	0.0058	0.0012	<b>0.0459*</b>

\* Note that these values correspond to within-class variance.

## Figures:

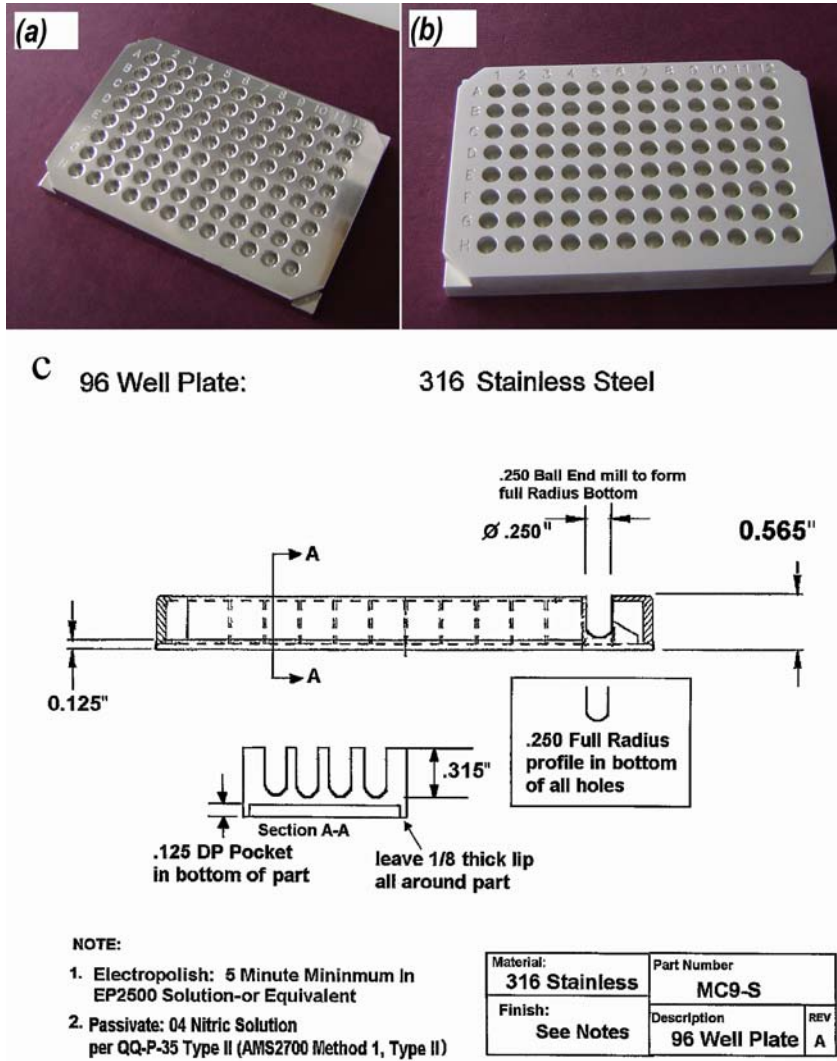


**Figure 1:** Photographs of the metal 96 multi-well plates used in this study: (a) stainless steel, (b) aluminium, and (c) detailed engineering drawing of the stainless steel sample holder, showing the size and profile of the individual wells.

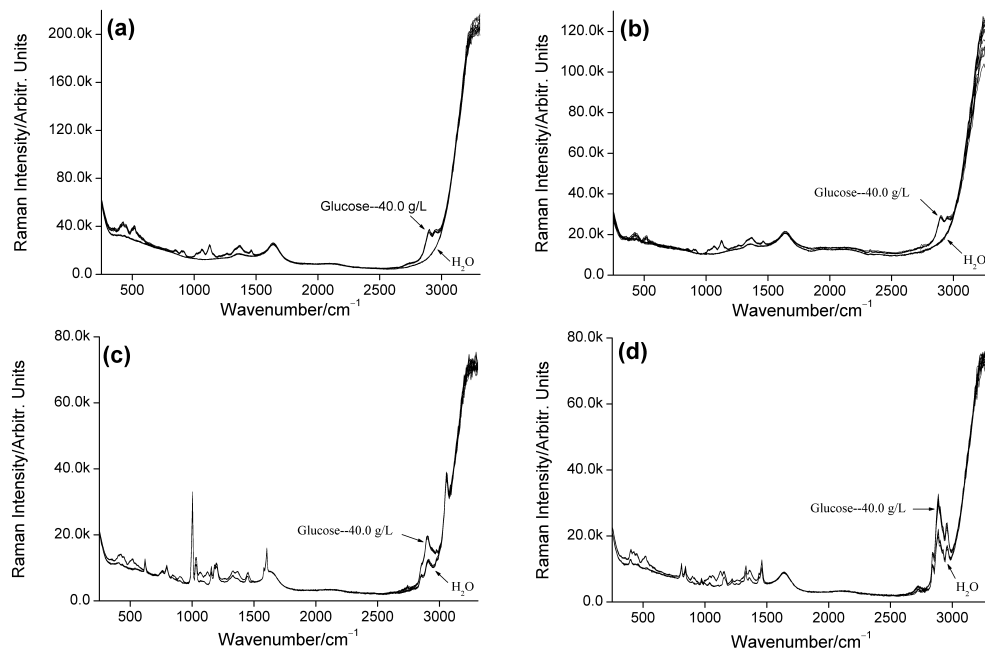


**Figure 2:** Raman spectra of water and glucose solution (40.0 g/L) collected in multi-well plates (MWP) fabricated from: (a) electropolished stainless steel, (b) hard anodised aluminium, (c) polystyrene, and (d) polypropylene.

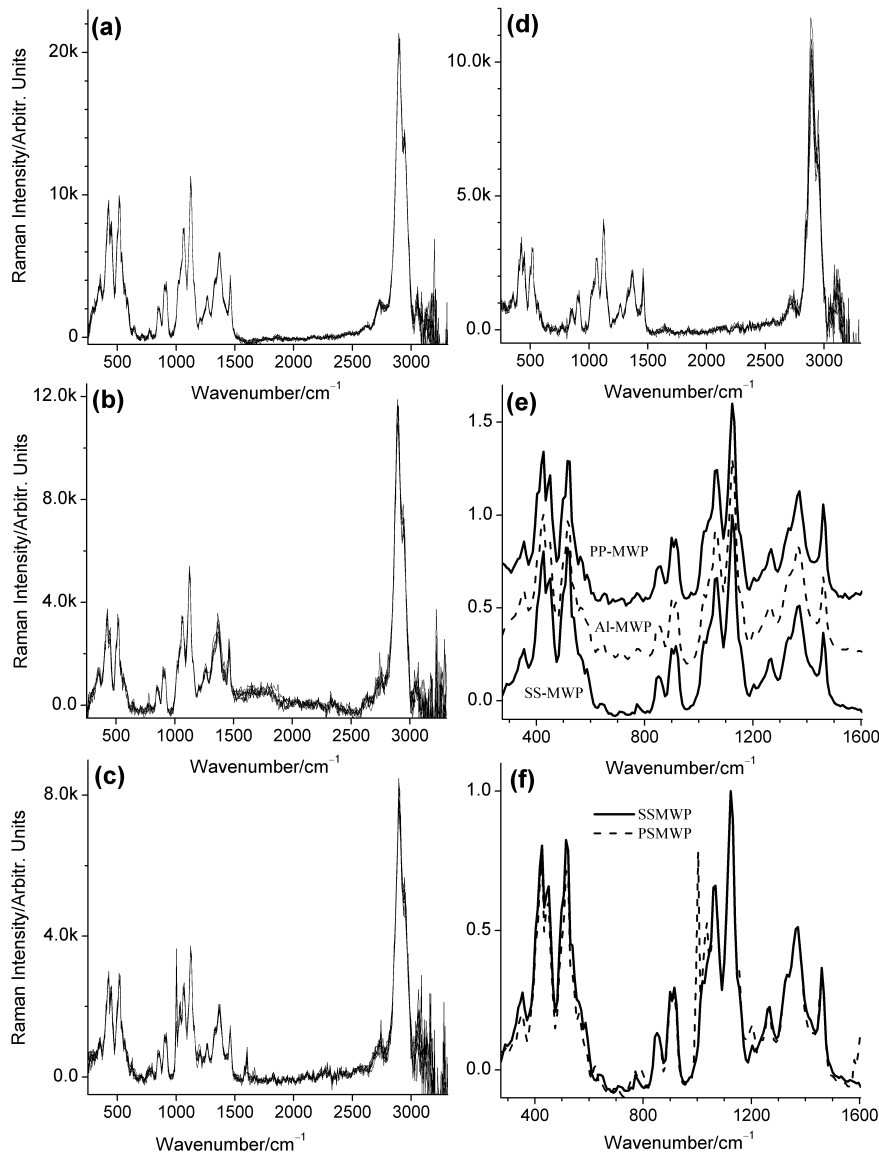


**Figure 3:** Background-subtracted, averaged, and normalised Raman spectra of glucose solutions (40 g/L) collected from the different multi-well plates: (a) stainless steel MWP, (b) aluminium MWP, (c) polystyrene MWP, and (d) polypropylene MWP. (e) and (f) Comparison of the background-subtracted Raman spectra within the 274~1604  $\text{cm}^{-1}$  region of interest (spectra in (e) are offset for clarity).

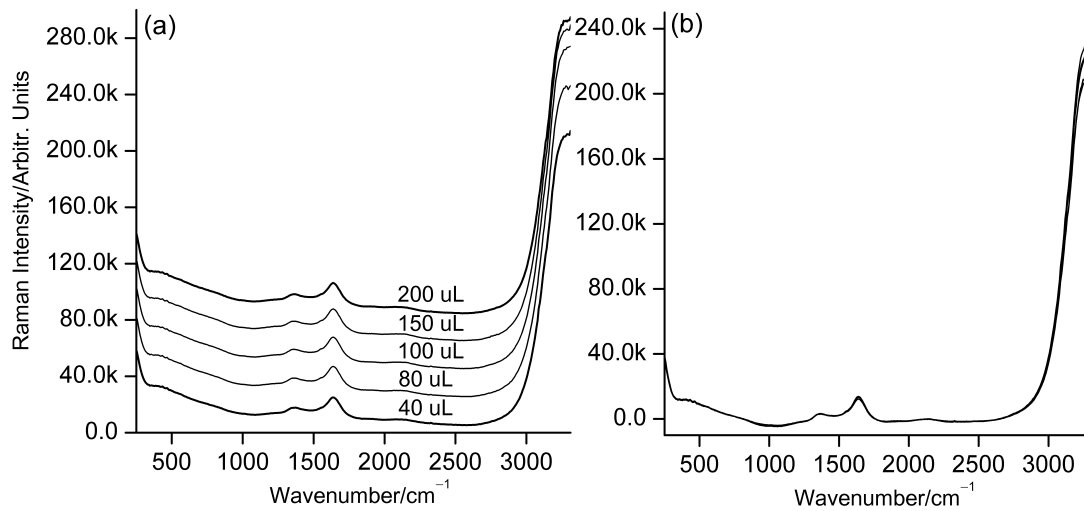


**Figure 4:** Raman spectra of water taken using the SS-MWP: (a) original spectra, where spectra were offset by a value of  $2 \times 10^4$  for clarity, and (b) baseline corrected spectra.

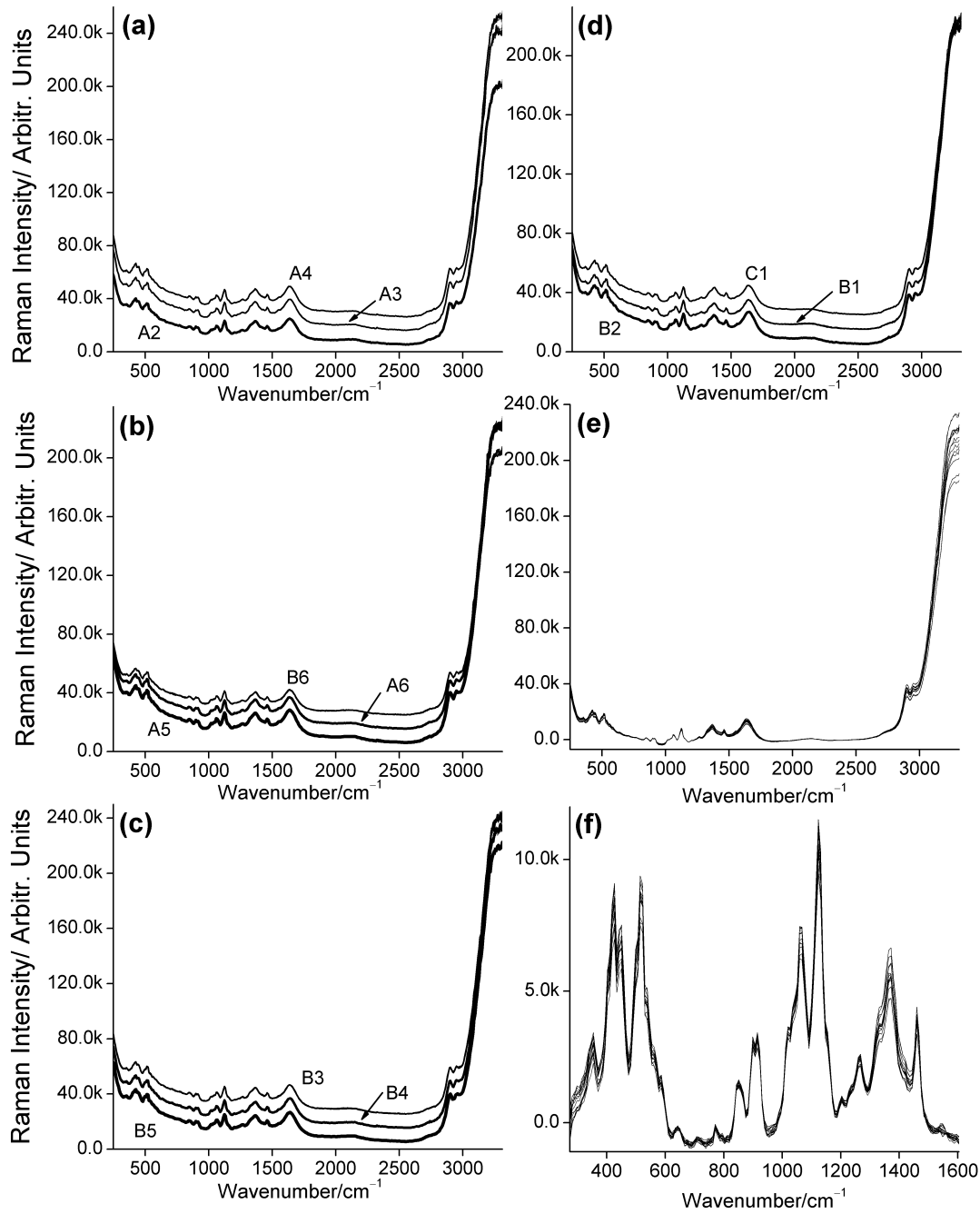


**Figure 5:** Raman spectra of 40 g/L glucose solutions taken from three different wells of a SS-MWP: (a) 40  $\mu$ L, (b) 80  $\mu$ L, (c) 100  $\mu$ L, (d) 150  $\mu$ L, (e) overlay of baseline corrected spectra, from all the measurements after averaging, in the 250~3311  $\text{cm}^{-1}$  region, and (f) overlaid background-subtracted spectra in the 274~1604  $\text{cm}^{-1}$  region. Note, for clarity, spectra were offset (by a value of  $10^4$ ) in plots (a) to (d).

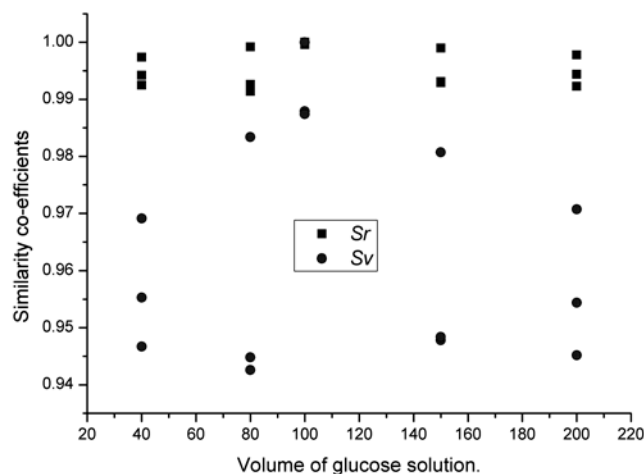


**Figure 6:** Plot of similarity coefficients versus volume of glucose solution (fixed concentration) taken from different wells on SS-MWPs. Values calculated using the background subtracted Raman spectra (274~1604  $\text{cm}^{-1}$  region) compared against a 100  $\mu\text{L}$  reference measurement.

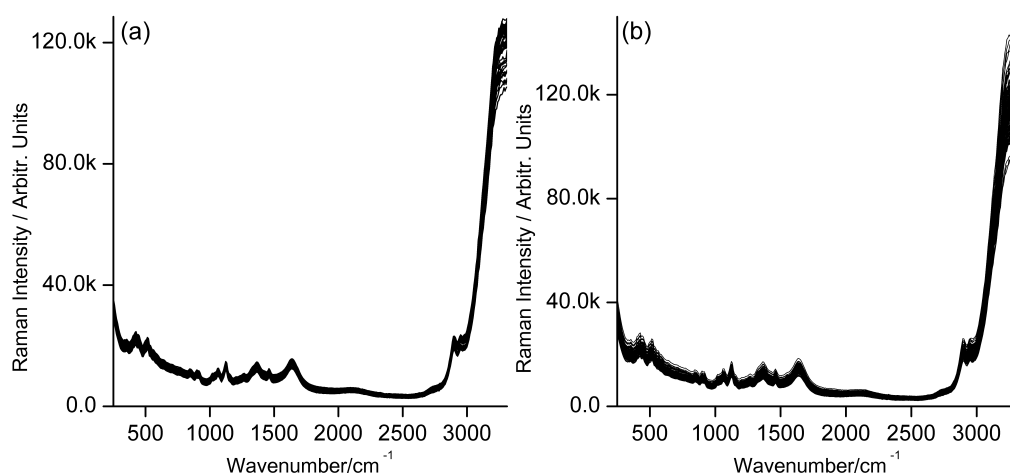


**Figure 7:** Raman spectra of glucose solution (40.0 g/L) collected in, (a) 40 random wells of an individual SS-MWP, and (b) 120 random wells of three individual SS-MWPs.

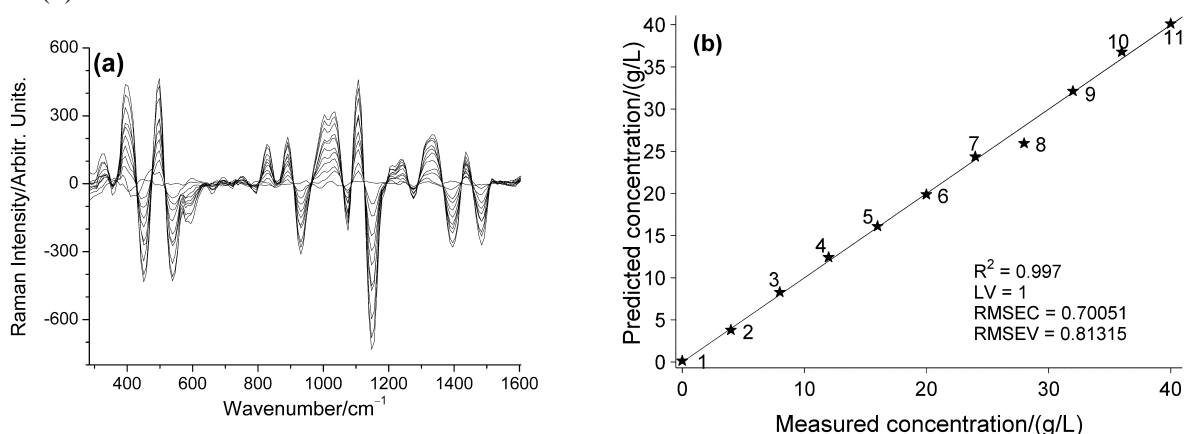


**Figure 8:** Overview of the linearity test for stainless steel plates using glucose solutions: (a) Raman spectra after sequential baseline correction, background subtraction and first order derivatization, and (b) predicted versus measured plot for glucose concentration predicted by the PLS model using one principal component. Diagonal line represents theoretically correct predictions.